01 May 2013, 8:45 am - 9:30 am

Keynote Address

W. D. Liam Finn
University of British Columbia, Canada

Guoxi Wu
BC Hydro, Canada

Commemorate the Legacy of Ralph B. Peck
April 29 - May 4, 2013 CHICAGO
Seventh International Conference on
Case Histories in Geotechnical Engineering
and Symposium in Honor of Clyde Baker

DYNAMIC ANALYSES OF AN EARTHFILL DAM ON OVER-CONSOLIDATED SILT WITH CYCLIC STRAIN SOFTENING

W.D. Liam Finn
University of British Columbia
6250 Applied Science Lane, Vancouver, BC, Canada

Guoxi Wu
BC Hydro
6911 Southpoint Drive, Burnaby, BC, Canada, V3N 4X8

ABSTRACT

This paper describes a study of the John Hart earthfill dam on Vancouver Island in British Columbia, Canada, under very strong shaking. The study has two quite interesting features. Firstly the dam is founded on over-consolidated silt that strain softens with cycles of strong shaking, leading to significant cyclic mobility problems. Secondly BC Hydro in addition to its own internal analyses using a finite element program (VERSAT), commissioned external confirmatory analyses by an outside consultant using a different program (FLAC) and constitutive model. The two analyses predicted different deformation patterns in the downstream slope for crustal earthquakes.

INTRODUCTION

This paper describes a study of the seismic response analysis of the John Hart earthfill dam on Vancouver Island in British Columbia, Canada, under very strong shaking. The dam is owned by BC Hydro. The primary objective of the study is to provide a data base to guide selection and implementation of measures to mitigate deficiencies in the dam.

The study has two quite interesting features. Firstly the dam is founded on over-consolidated silt that strain softens with cycles of strong shaking, leading to significant cyclic mobility problems. Secondly for this study BC Hydro required that in addition to its own internal analyses, external confirmatory analyses should be conducted by outside consultants using a different program and constitutive model.

The internal analyses were conducted using the program VERSAT (Wu 2001 & 2012). VERSAT is a modification of the program TARA-3 (Finn et al. 1986) that has been used in analyses of about 20 major earthfill dams. The principal modifications are the introduction of an additional pore water pressure model based on Seed's cyclic stress approach (Seed et al. 1976), a modification of the loading/unloading routine to ensure a better fit with the modulus degradation curves and strain dependent damping ratios used in equivalent linear analyses, and a dilative silt model. Preliminary external analyses were conducted with the finite difference computing platform FLAC (Itasca 2008) using the UBC SAND and UBC HYST Models (Beaty and Byrne 1998; Naesgaard and Byrne 2007). The two analyses predicted different ground deformation patterns in the downstream slope for crustal earthquakes.

JOHN HART MIDDLE EARTHFILL DAM

The John Hart Dam is located 9 km west of the City of Campbell River, British Columbia, Canada. The dam was constructed between 1946 and 1947 on the Campbell River. The main components of the John Hart Development consist of:

- a 250 m long and 30 m high concrete gravity dam with a three bay gated spillway;
- north, middle and south earthfill dams 200 m, 350 m and 50 m long, respectively;
- a 10 m high concrete intake structure with six gated bays; and
- three 3.66 m diameter and 1.8 km long wood stave/steel penstocks connecting to the downstream powerhouse.

Campbell River is located on Vancouver Island, an area of high seismicity where two earthquakes of M7 or greater have

been recorded within the last century. The first recorded earthquake occurred in 1918 off the west coast of Vancouver Island with a magnitude of 7.0. The second recorded earthquake, with a magnitude of 7.3, occurred in 1946 within 30 km of the John Hart Dam, which was under construction at that time. The Cascadia subduction zone, located off the west coast of Vancouver Island and with a potential earthquake magnitude of 9.0 – 9.2, is about 110 to 125 km away from the dam site.

The Middle Earthfill Dam

An aerial view of the John Hart Dam Middle Earthfill Dam is shown on Fig. 1, which also shows the intake structure and a portion of the penstocks. The Middle Earthfill Dam, about 350 m long and up to 20 m high, is located between the power intake and the concrete dam. From 1987 to 1988, a major seismic upgrade was completed at the Middle Earthfill Dam to improve its seismic performance. The 1987/1988 seismic upgrade included placement of rockfill, sand and gravel (vibro-compacted) in the upstream, construction of a slurry trench cut-off wall and a downstream earthfill dam which includes a 3 m thick drain/filter layer at its base and a 3 m impervious core within the pervious shell.

Soil data collected in the site investigation works carried out between 1985 and 1988, were used to develop the soil model and strength parameters for the analyses. The data included stratigraphy logging, field vane shear tests, SPT blow counts (N values with hammer energy measurements), grain size curves, and index test results from a total of 80 mud rotary SPT holes drilled within the Middle Earthfill Dam area. In addition, data from Cone Penetration Tests (CPTs) were also used in the determination of soil parameters.

A simplified cross section of the Middle Earthfill Dam is shown in Fig. 2. The dam fills and foundation subsoil are grouped into the following soil units:

- Rockfill: The rockfill dyke was placed at a side slope of 1.3H:1V for a crest width of 6 m.
- Sand & Gravel Fill: Placed immediately behind the rockfill after the rockfill dyke was constructed. The sand and gravel fill was then densified using the vibro-compaction method. Becker penetration tests (BPT) in 56 holes after densification indicated that the densified materials were very dense with an estimated equivalent SPT $(N_1)_{60}$ of 51 between a depth of 5 to 15 m where a majority of the BPTs were performed.
- New Dam Fill: The new dam fill was placed and compacted in layers after the ground excavation was completed and consists of a sand and gravel shell, a 3 m thick impervious fill zone, a drain layer, a filter zone and a rockfill toe.
- Gully Sand: The Gully Sands were densified together with the sand and gravel fill. Thus in the soil model the Gully Sands were treated as part of the compacted sand & gravel fill.
- Unit 2 (interbedded Silt and Sand): This unit was deposited in a very complex sedimentary environment. Thickness of the sand beds varies significantly within the unit, from a sand seam to several meters in thickness. Under dynamic cyclic loads, this soil unit is modelled as cohesionless soils or sandy soils based on the $(N_1)_{60}$ values. The interbedded silts and sands were generally silt-dominant. However, within the footprint of the upstream rockfill area, sand layers with little bedding are clearly identifiable between El. 118 to 122 m. The El. 120 m sand layers were separated from the interbedded silts and sands and classified as Unit 2a for the loose sand and Unit 2b for the medium dense sand. The three subzones of Unit 2 soils are shown in Fig. 2 as red (2a), orange (2b) and dark green (2c) in the vicinity of the slurry trench and underneath the rockfill.
- Unit 3 (dessicated Silt): A green - grey dessicated silt layer was encountered immediately above the El. 120 sand layers. The layer is generally thin and about 1 m in thickness.
- Unit 4b (sand & gravel): A very dense layer of sand and gravel was encountered underlying Unit 2 soils in a number of drill holes within the rockfill area.
- Unit 5 (Lower Silt): a massive grey silt layer with little evidence of bedding. White shell fragments and thin fine silty sand seams were occasionally found in the Lower Silt. The new dam is constructed entirely on top of this Lower Silt. In the analyses, the Lower Silt is divided into four major subzones: M12 above the ground water level, M13 with in-situ effective vertical stresses less than 250 kPa, M14 with stresses between 250 and 400 kPa, and M15 with stresses between 400 and 600 kPa.
- Unit 6 (Glacial Till): The Vashon Drift was found underlying the Lower Silt. This till consists of a bluish, grey, very dense concrete-like mixture of gravel in a sandy clay matrix. While the till surface is well defined in the area downstream of the slurry trench cutoff, there are insufficient soil data to define the surface elevations of the till in the area upstream of the cutoff. The upstream till surface shown in the soil models is inferred from the available soil data.

Cyclic DSS Tests on Lower Grey Silt

In order to provide site specific data on seismic or cyclic behavior of the Lower Silt, a laboratory testing program was carried out by BC Hydro in 2012.

Three boreholes (BH12-08, BH12-09 and BH12-10) were drilled on the lower bench (El. 117.5 m in Fig. 2) of the Middle Earthfill Dam. A total of twelve thin-walled tube samples ("Shelby tubes") were collected from BH12-09 in the Lower Silt by the Piston Sampling Method. Five of the

Fig. 1 An aerial view of the John Hart Middle Earthfill Dam in British Columbia, Canada

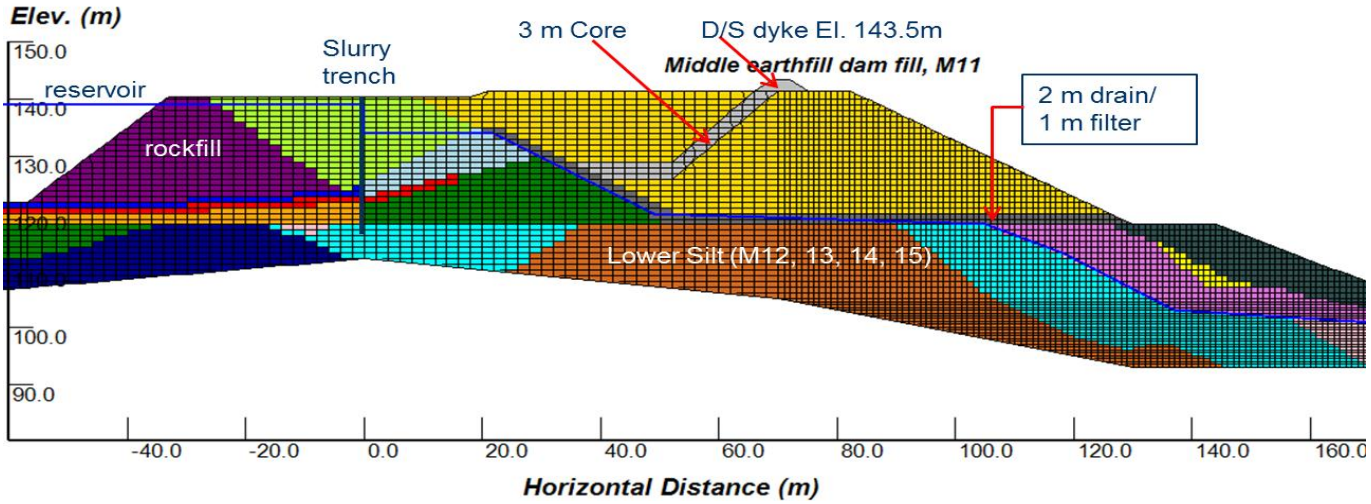

Fig. 2 A simplified cross section of the Middle Earthfill Dam

Shelby tubes (13A, 14A, 16 A, 18A and 20A, all below the water table at the lower bench) were selected for laboratory testing.

The laboratory tests completed in 2012 on the Lower Silt included the following:

- Five hydrometer tests and five Atterberg limits, one test for each tube. The Lower Silt consists of 70 – 80% silt size particles and 20 – 30% clay size particles; but it is classified as low plasticity clay (CL) on the Casagrande plasticity chart (Fig. 3).
- Three Constant Rate Strain (CRS) consolidation tests;
- Two Isotropic Consolidated Undrained (CIU) triaxial tests;
- Seven Static Direct Simple Shear (static DSS) tests;
- Seventeen Cyclic Direct Simple Shear (cyclic DSS) tests.

For both static and cyclic DSS tests, the sequence of applying vertical consolidation loads prior to shearing is as follows:

- Apply a seating pressure of 5 kPa and maintain it for one hour.
- Increase the vertical stress by increments to the

testing vertical stress (σ'_{vo}), maintain it for six hours, and record the settlements during consolidation.

- In some tests with testing OCR > 1.0, the vertical stress was further increased to the estimated pre-consolidation stress (σ'_p) and maintained for six hours, and then decreased back to the testing vertical stress level and maintained at this level for another six hours.

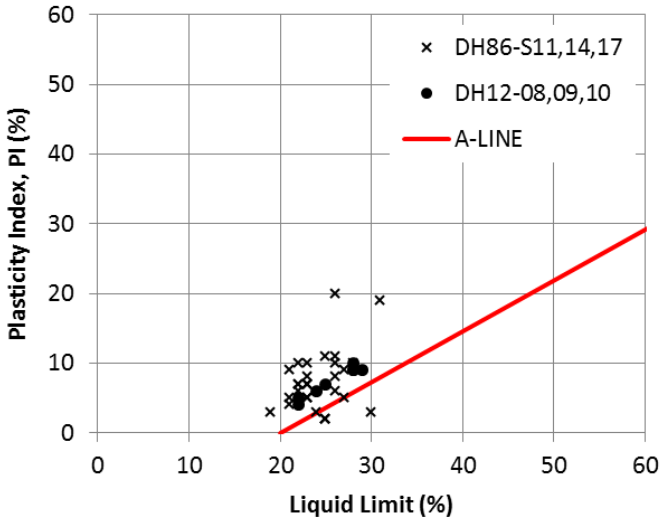

Fig. 3 Atterberg Limits for the Lower Silt

In static DSS tests, the samples were sheared after completion of consolidation to a maximum shear strain of 26% at a strain rate of 2% per hour. Four of the seven static DSS tests were conducted at a testing OCR of 1.0; and the remaining three tests were carried out at OCR's of 1.5, 2.3 and 3.25.

Nine of the 17 cyclic DSS tests were conducted with a testing OCR of 1.0, and the remaining eight tests were carried out with OCR=1.5 for six tests and OCR=2.3 for two tests.

In addition, cyclic DSS tests were carried out with and without a static shear stress bias. For tests with a static bias, a static shear load was applied under drained conditions over a period of two hours after vertical consolidation is completed.

After consolidation or static bias application is completed, cyclic shear stresses were applied under constant volume conditions with a frequency of 0.5 Hz until one of the following conditions was met:

- Minimum 5% single amplitude strain;
- 100% pore water pressure increase; or
- Maximum 150 cycles.

After completion of each cyclic loading test, the shear stress was brought back to zero (or static bias shear stress if applicable), and the post-cyclic sample was then sheared to a maximum shear strain of 20% to 25% at a strain rate of 5% per hour. Post-cyclic shear loading was applied in the same direction as unloading, or in the direction of static bias for tests with a static bias. At this point, the sample was returned to zero shear strain and reconsolidated, and changes in vertical displacement were recorded.

A cyclic test on 18A-CDSS2 was conducted at a testing OCR of 1.0 (σ'_{v0} 360 kPa and static bias 36 kPa). The sample started to show cyclic strain softening response after the shear strain reached about 5% in about 24 cycles, and developed large shear strains (in the order of 15 to 20%) only in only additional 5 cycles, as shown in Fig. 4.

A cyclic DSS test on 13A-CDSS5 was carried out at a testing OCR of 2.3 (σ'_{v0} 360 kPa and static bias 90 kPa). This sample also showed cyclic strain softening response after the shear strain exceeds about 5% and developed large strain in the order of 15% in about 15 cycles, as shown in Fig. 5. These two tests were conducted in order to investigate large strain cyclic response of the Lower Silt.

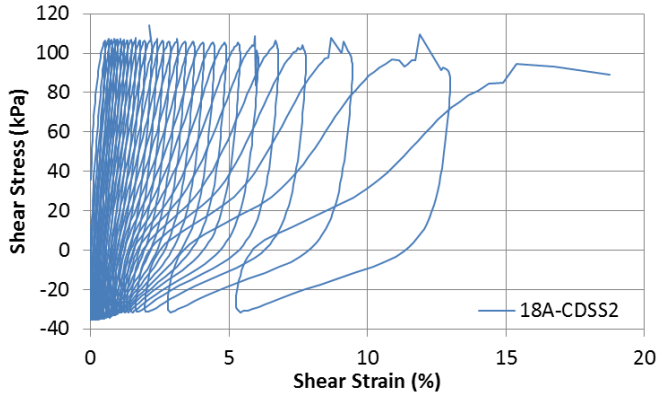

Fig. 4 Cyclic stress – strain response of 18A-CDSS2 (σ'_{v0}= 360 kPa, σ'_p= 360 kPa, OCR=1.0, static bias of 36 kPa)

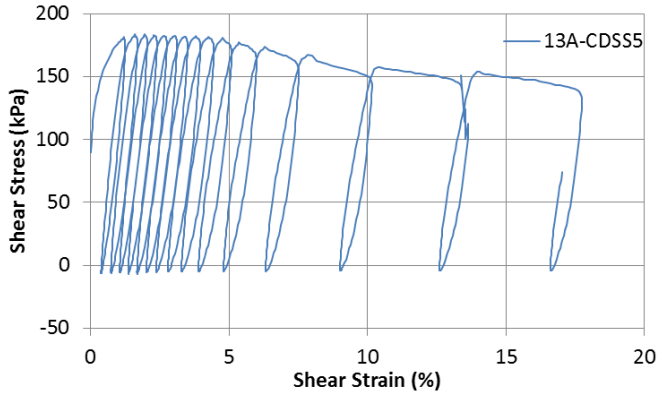

Fig. 5 Cyclic stress – strain response of 13A-CDSS5 (σ'_{v0}= 360 kPa, σ'_p= 830 kPa, OCR=2.3, static bias of 90 kPa)

Results of cyclic DSS tests on the over-consolidated Lower Silt confirmed that the cyclic resistance ratios (CRR), defined as cyclic stress ratio (CSR) to cause 5% shear strain, increases with OCR (Idriss and Boulanger, 2008). In order to target the

cyclic DSS tests to the in-situ OCR conditions, field pre-consolidation pressures of the saturated Lower Silt under the Middle Earthfill Dam were estimated first prior to the laboratory tests.

The in-situ pre-consolidation pressures (σ'_p) of the Lower Silt were estimated to be 825 to 1170 kPa from results of laboratory CRS consolidation tests. The undrained shear strengths (S_u) of the 1985 and 2012 field vane shear tests were also used to estimate σ'_p of the Lower Silt using empirical relationships of S_u and σ'_p, which results in σ'_p in the range of 700 to 1170 kPa.

Therefore, a pre-consolidation pressure of σ'_p= 830 kPa is considered to be conservatively representative of the in-situ conditions and thus was used to establish the OCRs in eight cyclic DSS tests. Cyclic Resistance Ratios (CRR, as defined earlier) from these cyclic DSS tests with a testing OCR of 1.5 (σ'_{v0}= 550 kPa) and 2.3 (σ'_{v0}= 360 kPa) are shown in Fig. 6, including results with and without a static bias (alpha=static bias/ σ'_{v0}).

Results of cyclic DSS tests on samples from P1-14 and P1-20 are also included in Fig. 6 for comparison. Borehole P1 was drilled in 2009 in the general area of John Hart Dam, and cyclic DSS tests were conducted on silt samples. The silt samples from P1-14 and P1-20 shown in Fig. 6 had similar PI values and stress conditions (i.e., σ'_p from 855 to 912 kPa) to the Lower Silt under the Middle Earthfill Dam.

The cyclic DSS tests revealed the following:

- Cyclic resistance ratio (CRR), i.e., CSR to cause 5% shear strain, in the Lower Silt increases with over-consolidation ratio (OCR);
- Initial static shear stress, i.e., static bias, significantly reduces the CRRs of the Lower Silt;
- These test results formed the basis for dynamic analyses that follow.

Dynamic Analyses of the Middle Earthfill Dam

After completion of the laboratory tests, BC Hydro started a study to update the seismic performance assessments of the Middle Earthfill Dam. As the work on determination of seismic parameters for the dam site, including input ground motion, is still in progress, dynamic time-history analyses of the dam were conducted with preliminary to understand the potential response mechanism of the dam to strong earthquake loading.

Dynamic time-history analyses of the Middle Earthfill Dam were carried out primarily using the finite element method with the computer program VERSAT-2D version 2012 (Wu 2012) and checked by an outside consultant using the finite difference method with FLAC version 6.0 (Itasca 2008).

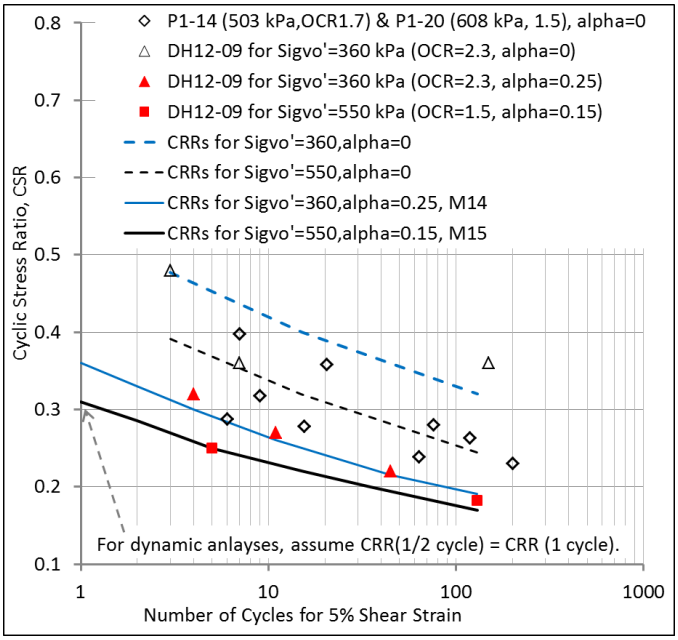

Fig 6 Cyclic resistance of over-consolidated Lower Silt from cyclic DSS tests

Input Ground Motions for Preliminary Analyses

A total of five acceleration or velocity time histories, recorded from past earthquakes, were selected as input ground motions for the dynamic analyses; and they were linearly scaled to fit a tentative target response spectrum. These earthquake ground motions consist of three records from crustal earthquakes and two records from subduction earthquakes as follows:

- 2011 Japan Tohoku M9.0 earthquake, record at MYG009 (Taiwa), EW component scaled by 1.16. This record was baseline corrected by BC Hydro after it was downloaded from the NIED K-Net database of Japan.
- 2010 Chile Maule M8.8 earthquake, record at Hualane, L component scaled by 1.06. This record was downloaded from a database provided by the Center for Engineering Strong Motion Data (CESMD).
- 1999 Taiwan Chi-Chi M7.6 earthquake, record at TCU071, W component scaled by 0.84
- 1994 US Northridge M6.7 earthquake, record at Chalon Rd, 070 component scaled by 2.18
- 1978 Iran Tabas M7.4 earthquake, record at Tabas, LN component scaled by 0.6

For both VERSAT-2D and FLAC dynamic analyses, the above input ground motions were applied as within motions at the bases of the finite element or finite difference models.

VERSAT-2D Finite Element Model

VERSAT-2D (Wu 2001&2012) is a 2-dimensional finite element program that is used to conduct dynamic stress and deformation analyses of earth structures subjected to base excitation or to dynamic loads at specified locations (Wu 2001; Wu and Chan 2002; Wu et al. 2006). The program includes a non-linear hyperbolic model to simulate the hysteresis response of soil under cyclic loads. Excess pore water pressures caused by cyclic loads, if applicable, can also be computed. Large ground displacements caused by excess earthquake loading are calculated using updated Lagrangian analysis. Structural beam elements and bar elements are used for modeling soil-structure interaction.

The program provides two options for applying the input ground motion. For a rigid-base model, the earthquake accelerations are applied at the base of model, and displacements relative to the model base are computed. Inertial forces on the soil mass caused by base motions are computed using Newton's law, and base accelerations are used directly in the equations of motions.

The equations of motions describing the incremental dynamic force equilibrium are given as:

$$[M]\{\Delta\frac{d^2\delta}{dt^2}\}+[C]\{\Delta\frac{d\delta}{dt}\}+[K]\{\Delta\delta\}=\{\Delta P\} \quad (1)$$

Where

[M] = mass matrices
[C] = viscous damping matrices
[K] = tangent stiffness matrices
[Δδ] = incremental displacement matrices
[Δdδ/dt] = incremental velocity matrices
[$\Delta d^2\delta/dt^2$] = incremental acceleration matrices
[ΔP] = incremental external load matrices

For a finite element model having an elastic base instead of a rigid base, outcropping velocity time histories are applied directly at the base of the model through a viscous boundary (i.e., energy absorbing boundary or elastic base boundary).

With acceleration input at the rigid base, incremental inertial forces on the soil mass caused by base accelerations are computed using the Newton's law and applied as [ΔP]. With the velocity input at the elastic base, incremental shear forces at the base nodes are determined and applied as [ΔP].

VERSAT-2D uses the hyperbolic stress - strain model to simulate the nonlinear and hysteresis shear stress - strain relationship for soils (Finn et al., 1977). The low-strain shear modulus, G_{max}, and the bulk modulus, B, are stress level dependent and computed as follows:

$$G_{\max}=K_g P_a(\frac{\sigma_m'}{P_a})^m \quad (2)$$

$$B=K_b P_a(\frac{\sigma_m'}{P_a})^n \quad (3)$$

Where

P_a = atmospheric pressure, 101.3 kPa
K_b = bulk modulus constant
K_g = shear modulus constant
m, n = shear modulus exponential, and bulk modulus exponential, respectively
σ_m' = effective mean normal stress from a static analysis.

The relationship between the shear stress, τ_{xy}, and the shear strain, γ, for the initial loading condition is modelled to be nonlinear and hyperbolic as follows:

$$\tau_{xy}=\frac{G_{\max}\gamma}{1+G_{\max}/\tau_{ult}\bullet|\gamma|} \quad (4)$$

Where

τ_{ult} = ultimate shear stress in the hyperbolic model

G_{max} = low-strain shear modulus ($G_{max}=\rho V_s^2$ with ρ being the soil density and V_s being the shear wave velocity).

The Masing criterion has been used to simulate the shear stress-strain relationship during unloading and reloading. The extended application of Masing criterion to irregular loading such as earthquake loading was also presented by Finn et al. (1977). However, a modification of the loading/unloading routine was introduced into VERSAT to ensure a better fit with the modulus degradation curves and strain dependent damping ratios used in equivalent linear analyses (Wu 2001, Wu 2010).

In addition to the hysteresis response, the stresses at each Gauss points in a finite element are continuously verified and corrected when necessary, so that they are consistent with the Mohr-Coulomb failure criterion.

Pore Water Pressure Models for Sandy Soils. The residual pore-water pressures are caused by plastic deformations in the sandy soil skeleton. They persist until dissipated by drainage or diffusion. Therefore they provide a great influence on the strength and stiffness of the sand skeleton. Hence during a dynamic time-history analysis, excess pore water pressures need to be continuously updated and their effects on soil strength and stiffness be continuously taken into account.

Three models are available in VERSAT-2D for computing the residual pore water pressures. The first two models are based on the cyclic shear strains to calculate the pore water pressures induced by cyclic loads (Martin et al. 1975). The third model determines the pore water pressure ratio, r_u, based on the equivalent number of uniform shear stress cycles (Seed et al. 1976) using the following relationship:

$$r_u=\frac{2}{\pi}\arcsin(\frac{N_{15}}{15})^{1/2\theta} \quad (5)$$

where θ is an empirical constant, and N_{15} is the equivalent number of uniform shear stress cycles. The following equation is used to convert shear stresses of irregular amplitudes, τ_{cyc}, to the uniform shear stress cycles:

$$N_{15} = (\frac{\tau_{cyc}}{\tau_{15}})^{\alpha} \quad (6)$$

where α is a shear stress conversion constant that is directly related to the magnitude scaling factor (MSF) (Wu 2001, Idriss and Boulanger 2008), and τ_{15} is the shear stress required to cause liquefaction in 15 cycles.

For the dynamic time-history analyses of John Hart Middle Earthfill Dam, Seed's pore water pressure model has been used for sandy soils (Units 2a, 2b and 2c) with α =1.4 which is consistent with the NCEER recommendations (Youd et al. 2001).

A summary of the key soil parameters developed for the dynamic analyses are presented in Table 1. Residual strengths (Sr/σ'_{vo}) of liquefied sandy soils were determined based on Idriss and Boulanger (2008). Shear wave velocities for the native soils were based on the measured shear wave velocities from seismic downhole investigations carried out in 1985 (DH85S-14, DH85S-17, DH85S-22, DH85S-25, and DH85S-28). K_{2max} values for fills were estimated using either empirical relationships or past project experience.

Calibration of Silt Model for the Lower Silt. The shear stress-strain relationship for the Lower Silt, that exhibit strain-softening but dilative characteristics after the pore water pressure exceeds a threshold value, is modelled in two phases using the Silt Model available in VERSAT-2D. When the pore water pressure ratio (r_u) is less than the threshold value, r_{u_0}, the hyperbolic stress-strain model described above for the sandy soils is used. When r_u exceeds the threshold value of r_{u_0}, a strain-softening but dilative model (Silt Model) is invoked in the analysis. The relationship between shear stress, τ_{xy}, and shear strain, γ, for the strain-softening but dilative condition, is assumed to be nonlinear and hyperbolic as follows:

$$\tau_{xy} = \frac{G_0 \gamma}{1 - |\gamma| / \gamma_{ult}} \quad (7)$$

Where

$$G_0 = [1 + \frac{12}{r_{u\_0}}(1 - r_u)]G_{liq} \quad (8)$$

$$\gamma_{ult} = \gamma_{H0} + \frac{r_u - r_{u\_0}}{1 - r_{u\_0}}(\gamma_H - \gamma_{H0}) \quad (9)$$

where γ_{H0} is ultimate shear strain (%) on initial strain softening for $r_u = r_{u\_0}$; γ_H is ultimate shear strain (%) at n^{th} cycle of strain softening for $r_u = 1.0$; and G_{liq} is initial shear modulus at n^{th} cycle of strain softening, i.e., liquefaction of silts at r_u=1.0. Assuming r_{u_0} of 0.3, the initial shear modulus G_0 on initial strain softening ($r_u = r_{u\_0}$) is determined to be $G_0 = 29\ G_{liq}$.

For the Silt Model, the dynamic pore water pressure ratio (r_u) is a model parameter for simulation of stress and strain response of a silt. Although all three dynamic pore water pressure models developed for the sandy soils are available for the Silt Model, the Seed's pore water pressure model was selected for simulation of the Lower Silt. The following model parameters for the Seed's model were derived from results of cyclic DSS tests shown in Fig. 6:

- CRR_{15} of 0.28, 0.25 and 0.22 for M13, M14, and M15, respectively. CRR_{15} is the CSR required to cause large cyclic shear strain (>5%) in 15 uniform cycles;
- Shear stress conversion constant of α = 8.0.

The parameters r_{u_0}, γ_{H0}, and γ_H are the Silt Model parameters used to control strain magnitudes, and they were determined by fitting response to cyclic test stress and strain data. An example of the model calibration is shown in Fig. 7 for a level ground condition with zero initial static shear stress.

For current analyses, calibration of the Silt Model for the Lower Silt was carried out for sloping ground conditions. The initial static shear stresses and in-situ OCRs for each subzone of the Lower Silt (i.e., M13, M14 and M15) were taken into considerations in the calibration. Results of the calibration indicated that r_{u_0}, γ_{H0}, γ_H of 0.3, 3.5% and 10%, respectively, were appropriate for the Lower Silt (M13, M14 and M15).

The shear stress – strain response from a calibration run for M14 of the Lower Silt (σ'_{v0}= 360 kPa, static bias 90 kPa) is shown in Fig. 8.

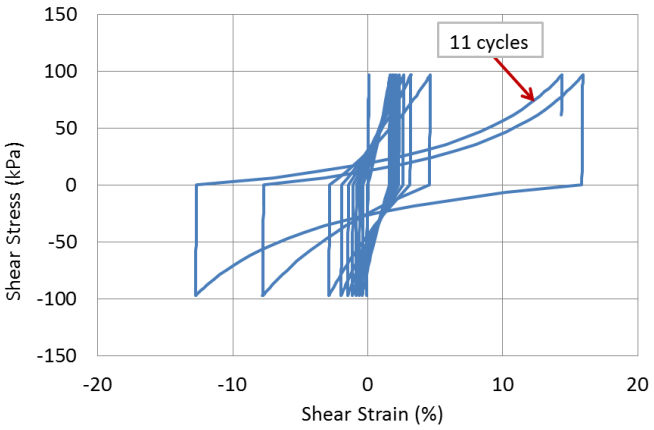

Fig. 7 An example of Silt Model calibration for a level ground condition with zero static shear stress

Results of VERSAT-2D Dynamic Analyses

The finite element model used for dynamic analyses of the Middle Earthfill Dam is shown in Fig. 9, and it consists of 7886 nodes, 7636 elements and 16 soil material zones.

Material Number	Soil Units Description	Elevation (m)	$(N_1)_{60}$ (30th Percentile)	FC (%) (30th Percentile)	$(N_1)_{60\text{-}cs}$ $=(N_1)_{60}+\Delta(N_1)_{60}$	$(N_1)_{60\text{-}sr}$	S_r/σ_{vo}'	Unit Weight (kN/m^3)	Cohesion (kPa)	Friction angle Φ (°)	V_s (m/s)	K_{2max} [2]
9	Rockfill	122 - 140.5	NA					20	0	40		120
8, 10	Sand&Gravel Fill (vibro-compacted)	122 - 140.5	51		Not liquefiable			20	0	38		74
11	New Dam Fill	118 - 141.5	NA					21	0	38		130
2	2a, Sand, some silt	120 - 121	10	< 5	10	10	0.09	19.6	0	35	300	
5	2b, Sand, some silt	118 - 120	26	< 5	26	26	0.28	19.6	0	35	300	
4	2c, Interbedded Silt and Sand	110 - 126	17	35 [1]	22	20	0.18	19.6	0	35	300	
3	3, Dessicated Silt	121 - 122	19		Not liquefiable			19.6	145	0	300	
6	4b, Sand & Gravel	? - 120	60					20	0	40	330	
12	5, Lower Silt, above water table	below 118	10		Not liquefiable			19.6	$114+0.16\sigma'_{vo}$	0	310	
13,14,15	5, Lower Silt, below water table	below 118	10		Based on results of 2012 cyclic DSS tests			20.5	$114+0.16\sigma'_{vo}$	0	310	
1	Organic Silt, below the lower bench	below 118	NA		Not liquefiable			19.6	50	0		37
16	Sand & Gravel Fill	below 118	NA		Not liquefiable			20	0	35		37
Base	6, Vashon drift (Till)	variable	Not required in model									

[1] FC=35% is assumed for Unit 2c/2d based on data from the Intake area

[2] $G_{max} = 217K_{2max}(\sigma'_m)^{0.5}$ where σ'_m is the effective mean stress in kPa; K_{2max} of 130 for the compacted new dam fill was based on measured V_s data from the Bennett Dam. K_{2max} 0f 74 for the compacted sand and gravel fill was estimated from the $(N_1)_{60}$ which was determined from 56 post-densification Becker Penetration Test Holes.

Table 1 Soil Parameters used in Dynamic Analyses of the Middle Earthfill Dam

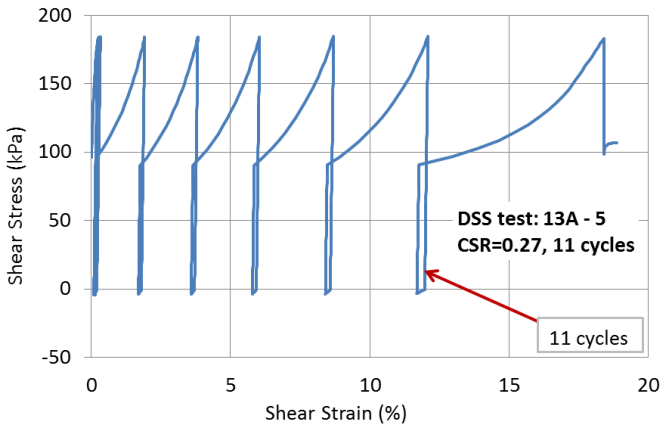

Fig. 8 A calibration run for M14 of the Lower Silt (σ'_{v0}= 360 kPa, static bias 90 kPa, r_{u_0}=0.3, γ_{H0}=3.5%, γ_H =10%)

Static shear stresses computed from a static stress analysis of the dam are shown in Fig. 10 in terms of their ratios to the effective vertical stresses. The static shear stress ratios in the Lower Silt (below El. 118 m) are generally less than 0.1 under the crest of the dam (x < 80 m); and they increase to 0.2 - 0.3 under the slope of the dam and below the lower bench (i.e., 80 < x < 160 m).

In a dynamic analysis, the factor of safety against soil liquefaction in the sandy soils or large cyclic strains in the Lower Silt is calculated by the program using N_{15} and α as defined in equation (6) as follows:

$$FS_{liq} = \left(\frac{15}{N_{15}}\right)^{\frac{1}{\alpha}} \qquad (10)$$

The FS_liq computed by the program indicates the cyclic resistance of soils such as the Lower Silt to the input ground motions; the loading from irregular earthquake motions (magnitude and duration) is converted to uniform stress cycles using the α parameter that is calibrated to results of cyclic DSS tests.

The factors of safety (FS_liq) computed from dynamic analyses are shown in Fig. 11 from the crustal Chi Chi input motion and in Fig. 12 from the subduction Tohoku input motion. The results showed that, under the subduction input motions, the entire saturated Lower Silt under the slope of the dam and below the lower bench would undergo large cyclic strains (>5%) with FS_liq <1.0; however, under the less severe crustal input motions, a portion of the saturated Lower Silt below the lower bench would not undergo large cyclic strains (or cyclic strain softening) with FS_liq > 1.1. As shown later, this zone in the Lower Silt with small cyclic strains has changed the ground deformation pattern of the Lower Silt slope under the crustal input motions.

The peak CSRs (ratio of peak cyclic stress to effective vertical stress) along a soil column at 110 m downstream of the slurry trench (i.e., x=110 m) are shown in Fig. 13 for all five input ground motions. The computed peak CSRs in the saturated zone of the Lower Silt (below El. 116.5 m) are in the order of 0.4 – 0.55, indicating very high loading demand from the seismic ground motions.

Fig. 14 shows a computed deformed mesh of the dam, with colored soil material zones, immediately after the earthquake using the Tohoku subduction ground motion. It is noted that very large deformations would occur on the upstream rockfill due to liquefaction of Unit 2a and 2b sandy soils. Along the

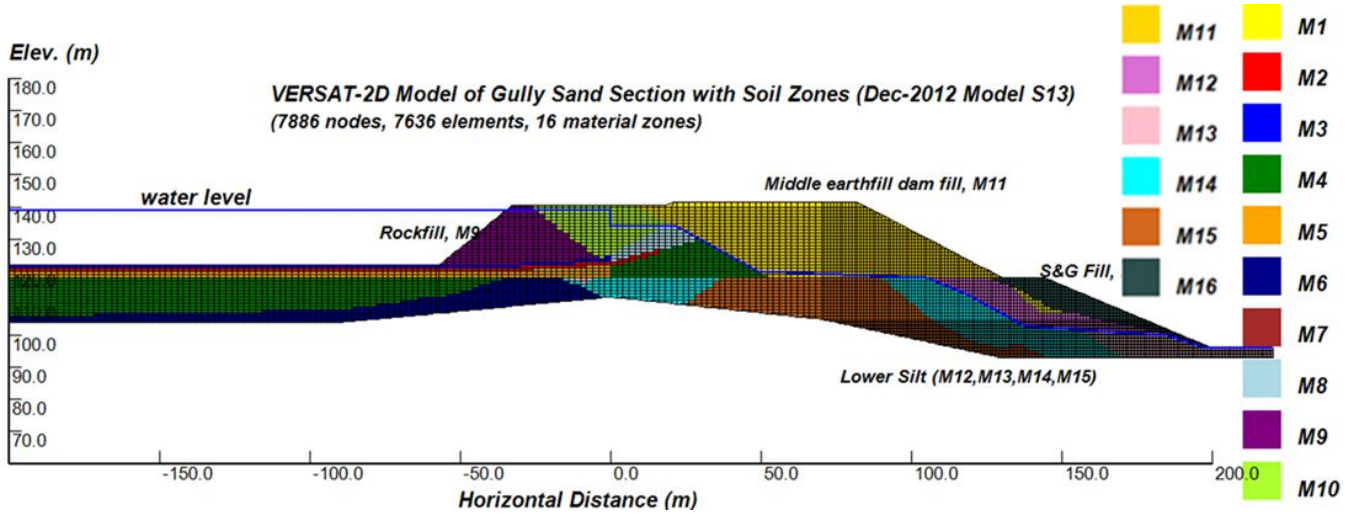

Fig. 9 VERSAT-2D finite element model showing soil material zones and ground water table of the Middle Earthfill Dam

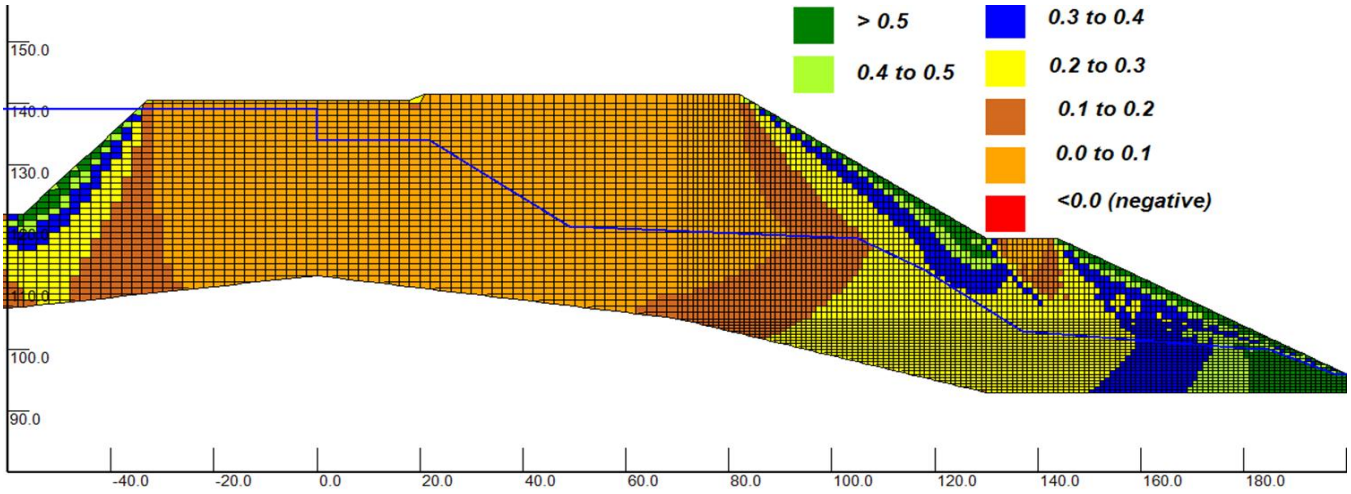

Fig. 10 Initial static shear stress ratios determined from a VERSAT-2D static stress analysis

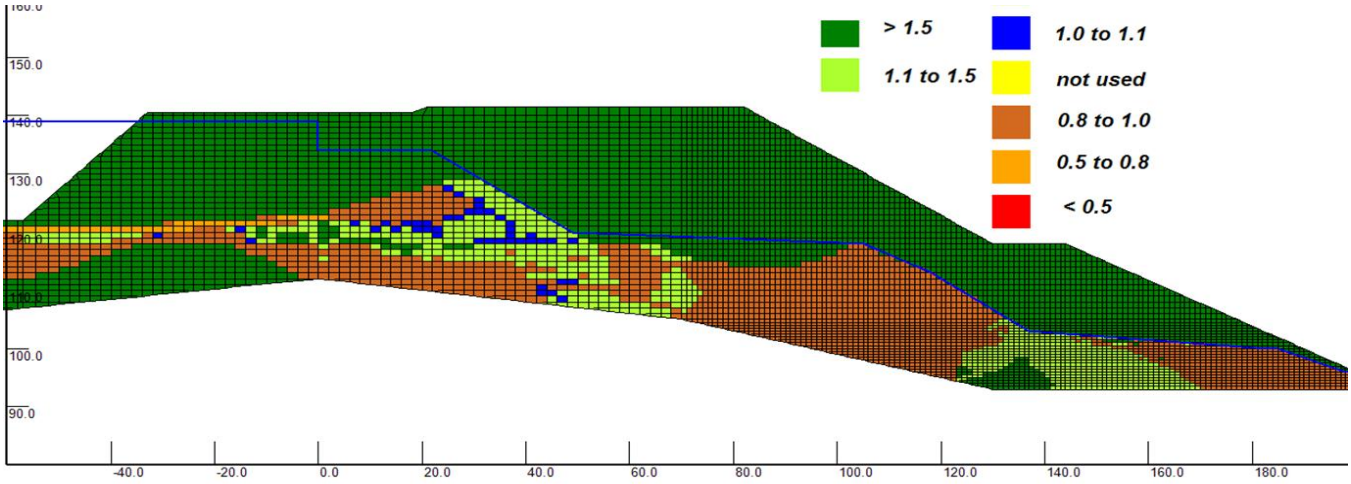

Fig. 11 Factors of safety against liquefaction or cyclic strain softening (FS_liq) from the Chi Chi crustal input motion

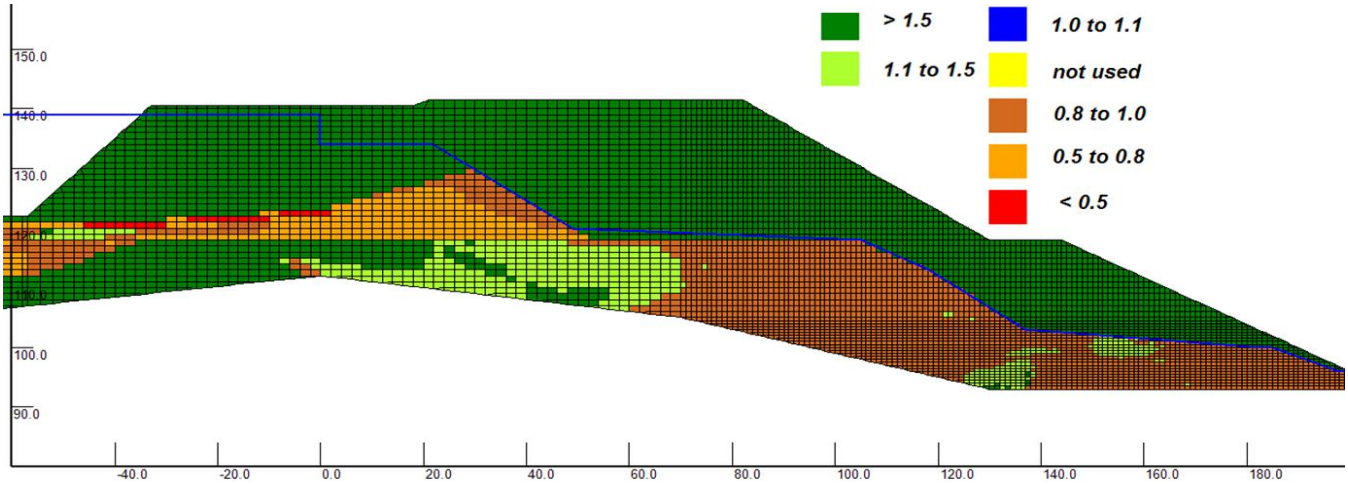

Fig. 12 FS_liq from the Tohoku MYG009 subduction input motion

downstream slope of the dam, deep seated large ground deformations and large shear strains (50 - 100%) would occur near the bottom of the Lower Silt as shown in Fig. 15 and Fig. 16, respectively.

However, deep seated sliding deformation was not predicted to occur under the crustal Chi Chi motion; instead, the sliding deformations break out at about 15 m above the bottom of the Lower Silt and through the relatively weak organic silt or fill along El. 108 m, as shown in Fig. 17. This shallow deformation pattern is primarily caused by the zone of small cyclic strains (FS_liq > 1.1) in the Lower Silt below the lower bench.

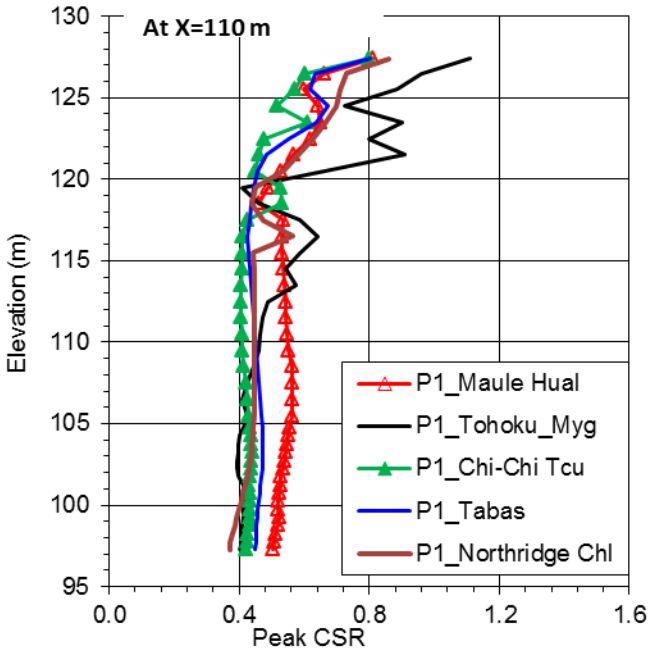

Fig. 13 Peak CSRs along a soil column at x=110 m from two subduction and three crustal input motions

Independent Check by FLAC

FLAC dynamic analyses were conducted by an external consultant to provide an independent check on dynamic analyses carried out by BC Hydro using the program VERSAT-2D. The dam cross section, soil material properties, and earthquake input motions were provided by BC Hydro.

Two dimensional non-linear dynamic numerical analyses were carried out using the finite difference program FLAC version 6.0 (Itasca 2008). The analyses were carried out in 'ground water mode' and flow and pore pressure redistribution was allowed. Saturated cohesionless (sandy) soils, and the saturated Lower Silt were modeled using a modification of the effective-stress constitutive model UBCSAND (Beaty and Byrne 1998), while very dense non-liquefiable granular soils (drained or free-draining) and the Unit 3 desiccated Silt were modeled using the total-stress Hysteretic Model UBCHYST (Naesgaard and Byrne 2007). In this context, 'effective-stress' refers to constitutive models where shear strain, skeleton volume change, and pore pressure are coupled and directly included in the model. In the 'total-stress' model, shear strain does not induce volume or related pore pressure change.

The FLAC numerical model used in dynamic analyses is shown in Fig. 18. The reservoir water with an elevation of 139.5m was included in the model using applied pressures to the surface of the reservoir bottom and dam. Earthquake velocity time history is applied at the model base for each input ground motion. Soil permeability used for various soil zones are shown in Fig. 19. The UBCSAND parameters for the Lower Silt were also calibrated using the cyclic DSS test results shown in Fig. 6.

Horizontal ground displacements of the dam at the end of the Chi Chi crustal motion are shown in Fig. 20; and displacements from the Japan Tohoku IMG subduction motion are shown in Fig. 21. The patterns of ground deformations

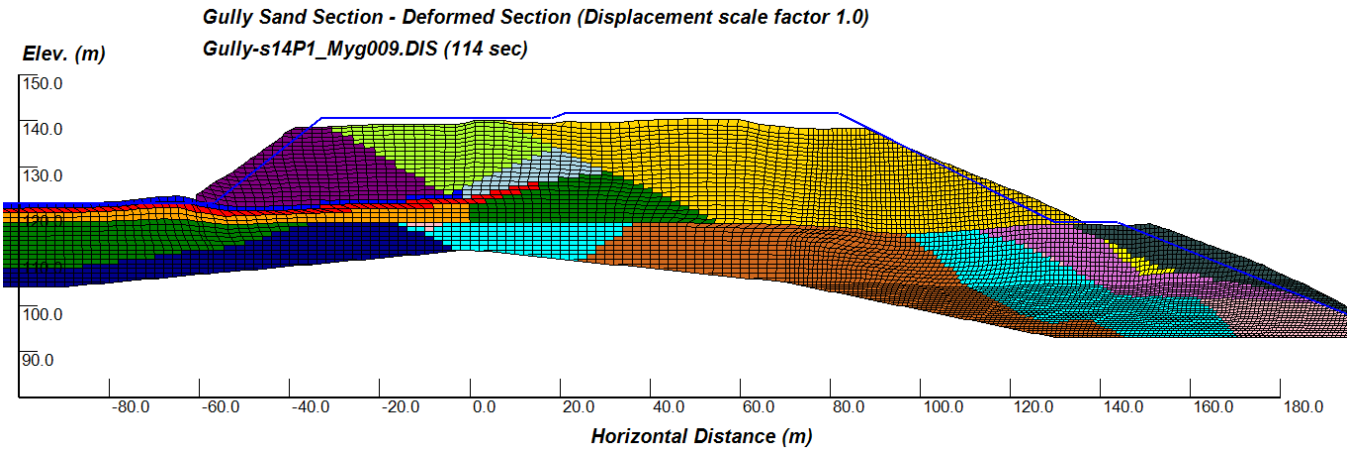

Fig. 14 A deformed cross section (with colored soil zones) computed from the Tohoku MYG subduction motion

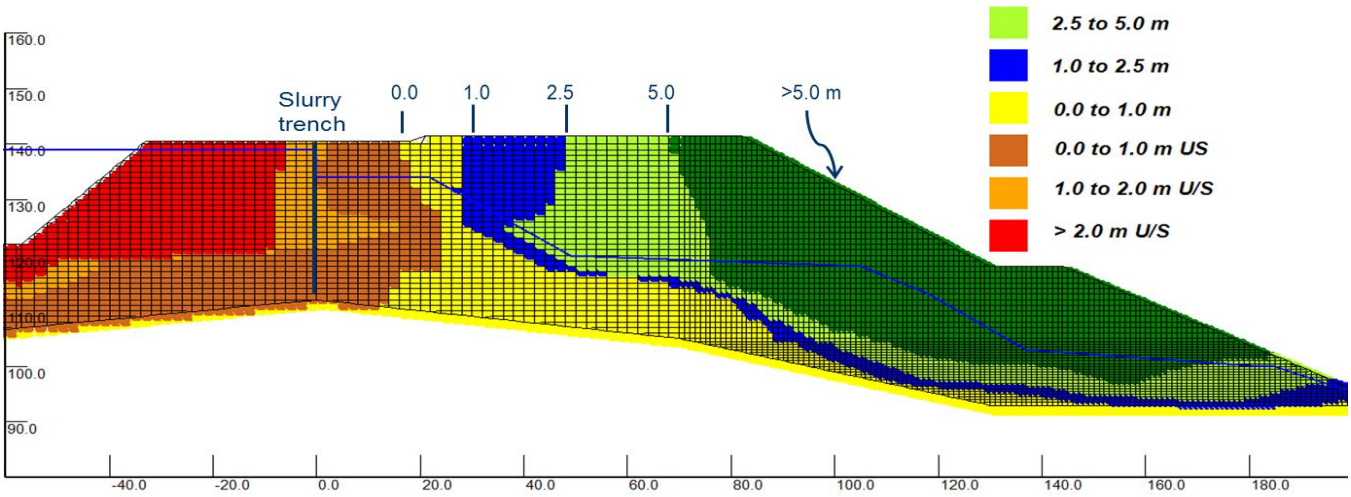

Fig. 15 Computed ranges of horizontal displacements from the Tohoku MYG subduction input motion

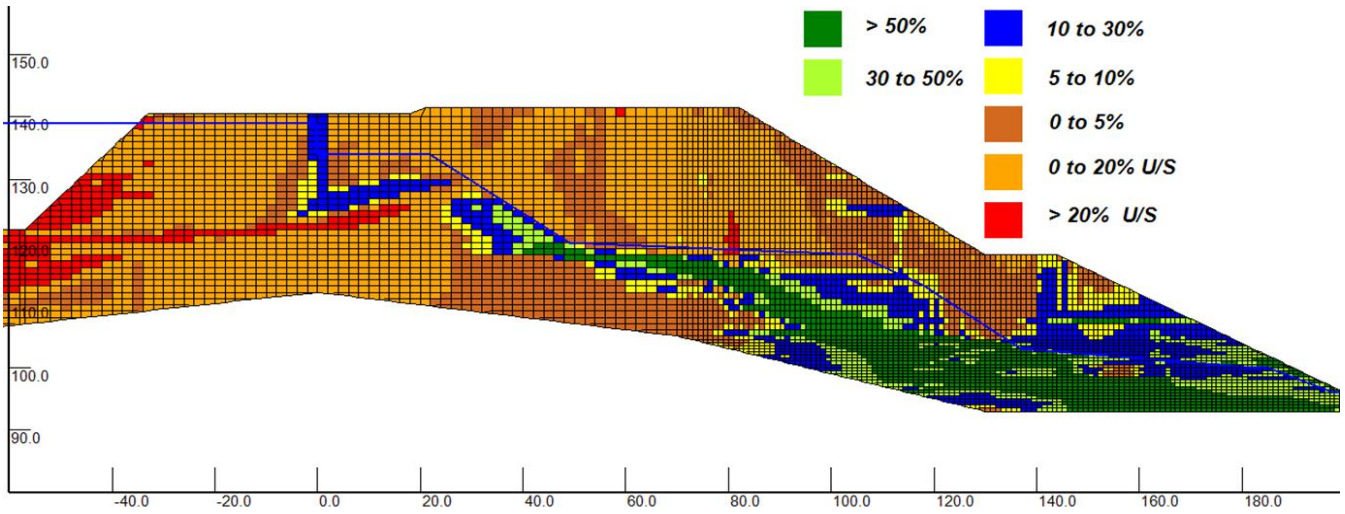

Fig. 16 A distribution of shear strains computed from the Tohoku MYG subduction input motion

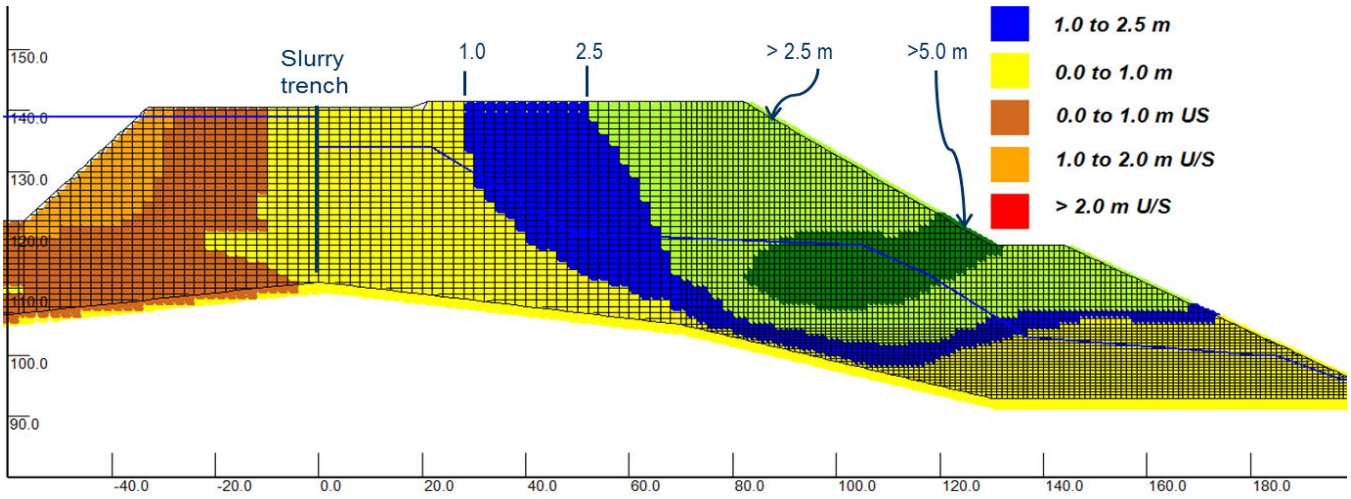

Fig. 17 Computed ranges of horizontal displacements from the Chi Chi crustal input motion

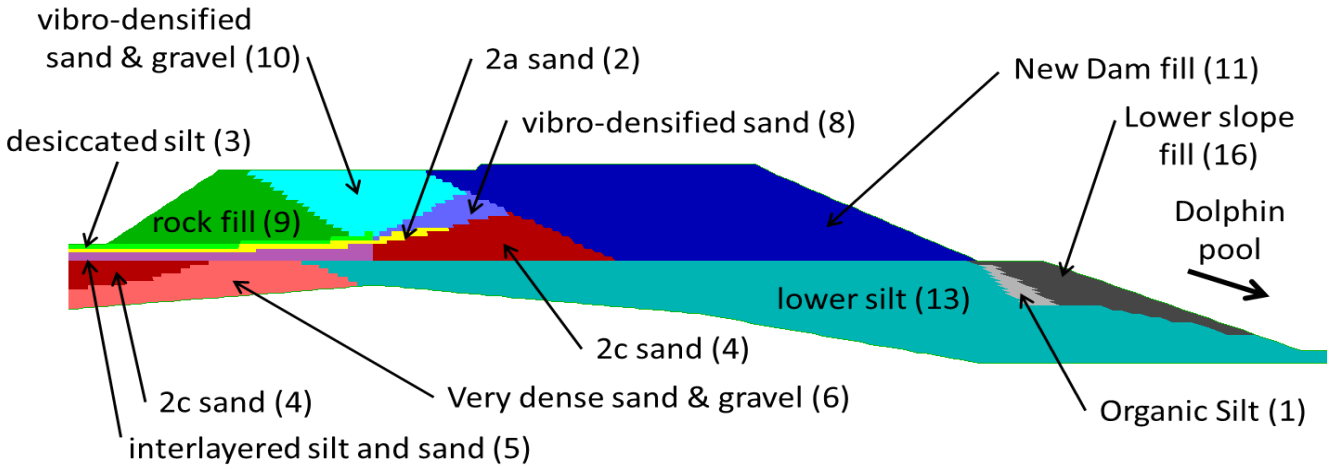

Fig. 18 A main portion of the FLAC model for the Middle Earthfill Dam

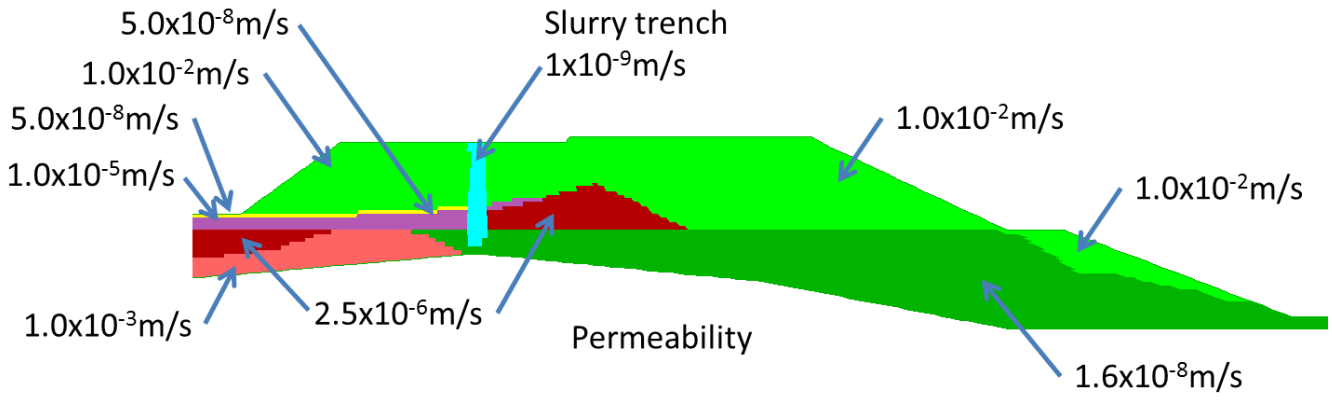

Fig. 19 Soil permeability used in FLAC groundwater flow mode

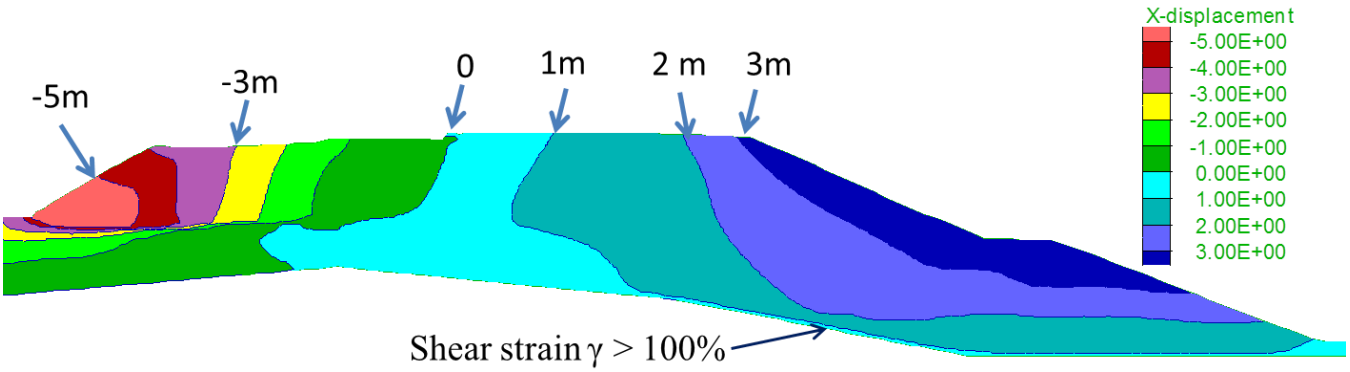

Fig. 20 FLAC preliminary results: Ranges of horizontal ground displacements from the Chi-Chi crustal input motion

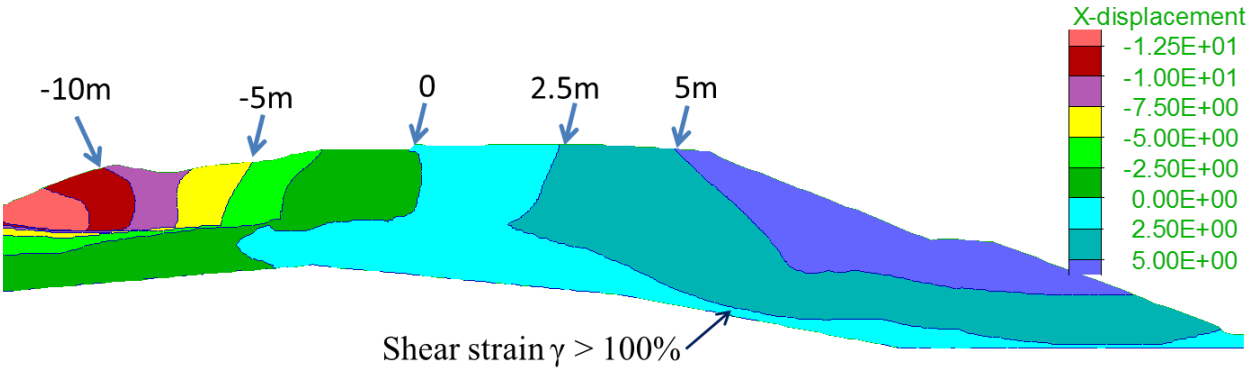

Fig. 21 FLAC preliminary results: Ranges of horizontal ground displacements from the Tohoku MYG subduction input motion

from the two input ground motions are similar; the subduction motion results in larger displacements as one would expect. Using the Chi Chi crustal motion, ground displacements were predicted to occur in excess of 1.0 m right at the base of the model, indicating shear sliding along the interface between the Lower Silt and the underlying hard ground (Till). Using the IMG subduction motion, the ground displacements in the same region increase to the order of 2.5 m.

Deep seated ground deformations are predicted by FLAC to occur for all five input ground motions. Fig. 22 shows a variation of shear strains with ground elevations along a soil column at x=110 m; it is seen that concentrations of large shear strain occur at the bottom of the Lower Silt. For Hualane and IMG subduction motions, the shear strains at the base are in the order of 200 – 400%; for Chi Chi (Tcu071) and Tabas crustal motions, they are in the order of 100 – 200%.

Summary of the Preliminary Dynamic Analyses

The preliminary dynamic analyses of the John Hart Middle Earthfill Dam results in the following:

- On the upstream of the dam, both programs predict similar patterns and magnitudes of ground deformations. Subjected to the subduction ground motions, the upstream rockfill dyke would deform in in the order of 5 to 10 m horizontally due to liquefaction of loose sandy soils under the dyke.
- The seismic response of the downstream earthfill dam, founded on the Lower Silt, appears to be more complex. There are two possible types of ground deformation patterns that can occur in the Lower Silt under the very strong earthquake loading.
- VERSAT-2D effective stress dynamic analysis predicts a relatively shallow ground deformation pattern for all three crustal ground motions. This is caused primarily by a zone of small cyclic strains in the Lower Silt below the lower bench.
- VERSAT-2D analysis predicts a deep seated ground deformation pattern for the two subduction ground motions as the strong and long duration motions have also triggered large cyclic strains (strain softening) of the saturated Lower Silt below the lower bench.
- FLAC soil-water coupled effective stress dynamic analysis predicts deep seated ground deformation pattern for all five input ground motions, similar to the response of one single rigid block seated on top

of the underlying hard or very stiff ground (Glacial Till).

DISCUSSIONS

This paper presents an interesting case history on dynamic time-history analyses of an earthfill dam founded on over-consolidated Lower Silt (PI generally less than 10%) subject to potentially very large earthquake loading. Laboratory cyclic direct simple shear tests confirmed that cyclic resistance of the Lower Silt increase with over-consolidation ratio (OCR); in addition, test results also showed that static shear stress bias can significantly reduce cyclic resistance of the Lower Silt.

In the dynamic time-history analyses using VERSAT-2D, calibration of the Silt Model for the Lower Silt was carried out using results of the cyclic DSS tests and taking into account the in-situ OCR and initial static shear stress conditions of the Lower Silt. While in FLAC dynamic analyses the UBCSAND model for the Lower Silt was also calibrated using the results of cyclic DSS tests, the two dynamic analyses give somewhat different ground deformation mechanisms on the downstream slope of the dam when subjected to the less severe crustal input ground motions.

These results suggest that it is advisable to check dam performance using by independent analyses using different programs and constitutive models.

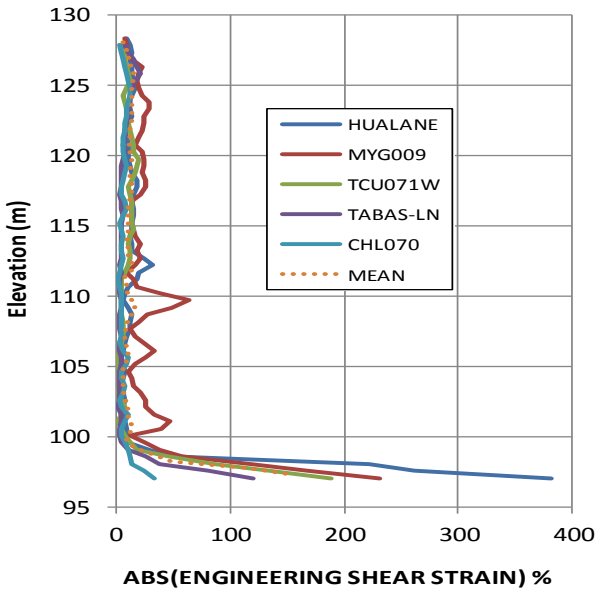

Fig. 22 Shear strains for a soil column at x=110 m from FLAC preliminary dynamic analyses

ACKNOWLEDGEMENTS

The authors would like to express their appreciation to BC Hydro for giving permission to publish soil data and preliminary results of the study on John Hart Middle Earthfill Dam and to BC Hydro colleagues and consultants for providing numerous suggestions and comments during the course of the work.

REFERENCES

Beaty, M. and P.M. Byrne [1998]. "*An effective stress model for predicting liquefaction behaviour of sand*", Geotechnical Earthquake Engineering and Soil Dynamics III. P. Dakou-las, M. Yegian, and R Holtz (eds.), ASCE, Geotechnical Special Publication 75 (1), pp. 766-777.

Finn, W.D.L, K.W. Lee and G.R. Martin [1977]. "*An effective stress model for liquefaction*". Journal of Geotechnical Engineering, ASCE, 103: 517-533.

Finn, W.D.L, M. Yogendrakumar, N. Yoshida and H. Yoshida [1986]. "*TARA-3: A program for nonlinear static and dynamic effective stress analysis",* Department of Civil Engineering, University of British Columbia, Vancouver, Canada.

Idriss, I.M. and R.W. Boulanger [2008]. "*Soil liquefaction during earthquakes*", Earthquake Engineering Research Institute, MNO-12

ITASCA, [2008]. "*FLAC version 6.0 Fast Langrangian Analysis of Continua User's Manuals*", Itasca Consulting Group Inc., Minneapolis Minnesota, USA.

Martin, G.R., W.D.L Finn and H.B. Seed [1975]. "*Fundamentals of liquefaction under cyclic loading*". Journal of Geotechnical Engineering, ASCE, 101(5): 423-438.

Naesgaard, E. and P.M. Byrne [2007]. "*Flow liquefaction simulation using a combined effective stress - total stress model*," 60th Canadian Geotechnical Conference, Canadian Geotechnical Society, Ottawa, Ontario, October.

Seed, H.B., P.P. Martin and J. Lysmer [1976]. "*Pore-water pressure changes during soil liquefaction*". Journal of Geotechnical Engineering, ASCE, 102(4): 323-346.

Wu, G. [2001]. "*Earthquake induced deformation analyses of the Upper San Fernando dam under the 1971 San Fernando earthquake*". Canadian Geotechnical Journal, 38: 1-15.

Wu, G., and S. Chan [2002]. "*Design of the Russ Baker Way Overpass on liquefiable sand - Vancouver Airport Connector - Sea Island, Richmond, BC*", Proceedings of the 6th International Conference on Short and Medium Span Bridges, Vancouver, pp. 579-586.

Wu, G., T. Fitzell, T and D. Lister [2006]. "*Impacts of deep soft soils and lightweight fill approach embankments on the seismic design of the Hwy. 15 North Serpentine River Bridges,*

Surrey, B.C", Proceedings of the 59th Canadian Geotechnical Conference, Vancouver, pp. 596-601.

Wu, G. [2010]. "*Seismic soil pressures on rigid walls with sloped backfills*", Proceedings of the 5th International Conference on Recent Advances in Geotechnical Earthquake Engineering and Soil Dynamics, San Diego, California, US, May 24-29.

Wu, G. [2012]. "*VERSAT-2D Version 2012, A Computer Program for Static and Dynamic 2-Dimensional Finite Element Analysis of Continua*". Wutec Geotechnical International, Vancouver, BC, Canada.

Youd, T.L. et al. (21 authors) [2001]. "*Liquefaction resistance of soils: Summary report from the 1996 NCEER and 1998 NCEER/NSF workshops on evaluation of liquefaction resistance of soils*". Journal of Geotechnical and Geoenvironmental Engineering, ASCE, 127(10): 817-833